4230–4240 *Nucleic Acids Research, 2013, Vol. 41, No. 7* *Published online 14 February 2013*
doi:10.1093/nar/gkt075

Unconventional miR-122 binding stabilizes the HCV genome by forming a trimolecular RNA structure

Stefanie A. Mortimer[1] and Jennifer A. Doudna[1,2,3,4,*]

[1]Department of Molecular and Cell Biology, University of California, Berkeley, CA 94720, USA, [2]Howard Hughes Medical Institute, University of California, Berkeley, CA 94720, USA, [3]Department of Chemistry, University of California, Berkeley, CA 94720, USA and [4]Physical Biosciences Division, Lawrence Berkeley National Laboratory, Berkeley, CA 94720, USA

Received November 30, 2012; Revised January 15, 2013; Accepted January 18, 2013

ABSTRACT

MicroRNAs (miRNAs) typically downregulate protein expression from target mRNAs through limited base-pairing interactions between the 5′ 'seed' region of the miRNA and the mRNA 3′ untranslated region (3′UTR). In contrast to this established mode of action, the liver-specific human miR-122 binds at two sites within the hepatitis C viral (HCV) 5′UTR, leading to increased production of infectious virions. We show here that two copies of miR-122 interact with the HCV 5′UTR at partially overlapping positions near the 5′ end of the viral transcript to form a stable ternary complex. Both miR-122 binding sites involve extensive base pairing outside of the seed sequence; yet, they have substantially different interaction affinities. Structural probing reveals changes in the architecture of the HCV 5′UTR that occur on interaction with miR-122. In contrast to previous reports, however, results using both the recombinant cytoplasmic exonuclease Xrn1 and liver cell extracts show that miR-122-mediated protection of the HCV RNA from degradation does not correlate with stimulation of viral propagation *in vivo*. Thus, the miR-122:HCV ternary complex likely functions at other steps critical to the viral life cycle.

INTRODUCTION

The liver-specific miRNA miR-122 is required for replication and translation of hepatitis C virus (HCV), a hepatotropic positive-sense RNA virus that can cause cirrhosis and hepatocellular carcinoma (1–3). Accounting for >50% of mature miRNAs in hepatocytes (4), miR-122 binds to the 5′UTR of HCV mRNA in infected cells and augments viral transcript stability and production of infectious virions (5). Although inhibition of miR-122 by anti-sense oligonucleotides is an effective anti-viral therapeutic strategy (6,7), the mechanism by which miR-122 enhances viral propagation remains incompletely understood.

Several lines of evidence suggest that miR-122 stimulates HCV infection by a mechanism that is distinct from miRNA-mediated attenuation of gene expression. Studies using mutated versions of miR-122 and HCV in cell culture revealed two binding sites for miR-122 near the 5′ end of the viral mRNA, in contrast to the typical location of miRNA binding sites within transcript 3′UTRs (8). Furthermore, both miR-122:HCV binding sites involve base pairing along the length of the miR-122 sequence, contrary to the predominant role of base pairing between nucleotides 2–8 at the 5′ end of miRNAs (the 'seed region') and their target mRNA binding sites (9,10) (Figure 1A). Finally, the miR-122:HCV interaction does not induce translational repression and/or deadenylation of the mRNA and does not trigger mRNA degradation, counter to the canonical effects induced by miRNAs (11,12). Importantly, miR-122 can function by this canonical pathway to downregulate host liver cell transcripts, primarily targeting genes involved in lipid and cholesterol metabolism (13–15). These observations suggest that HCV co-opts the host miR-122 to promote viral production by means of a distinct pathway (16,17).

Using a combination of biochemical and biophysical techniques, we show here that two copies of miR-122 bind simultaneously to the HCV 5′UTR but with unequal affinities. The resulting heterotrimeric interaction induces a stable structure that is distinct from the structure of the HCV 5′UTR alone. Although the miR-122:HCV structure resists degradation by the major cytoplasmic exonuclease Xrn1, this effect occurs even with mutant versions of miR-122 that do not enhance viral propagation in cell culture (9,10). This finding suggests that beyond direct stabilization of viral transcripts, the miR-122:HCV structure may recruit other viral or host factors or act to regulate other structures within the

*To whom correspondence should be addressed. Tel: +1 510 643 0225; Fax: +1 510 643 0080; Email: doudna@berkeley.edu

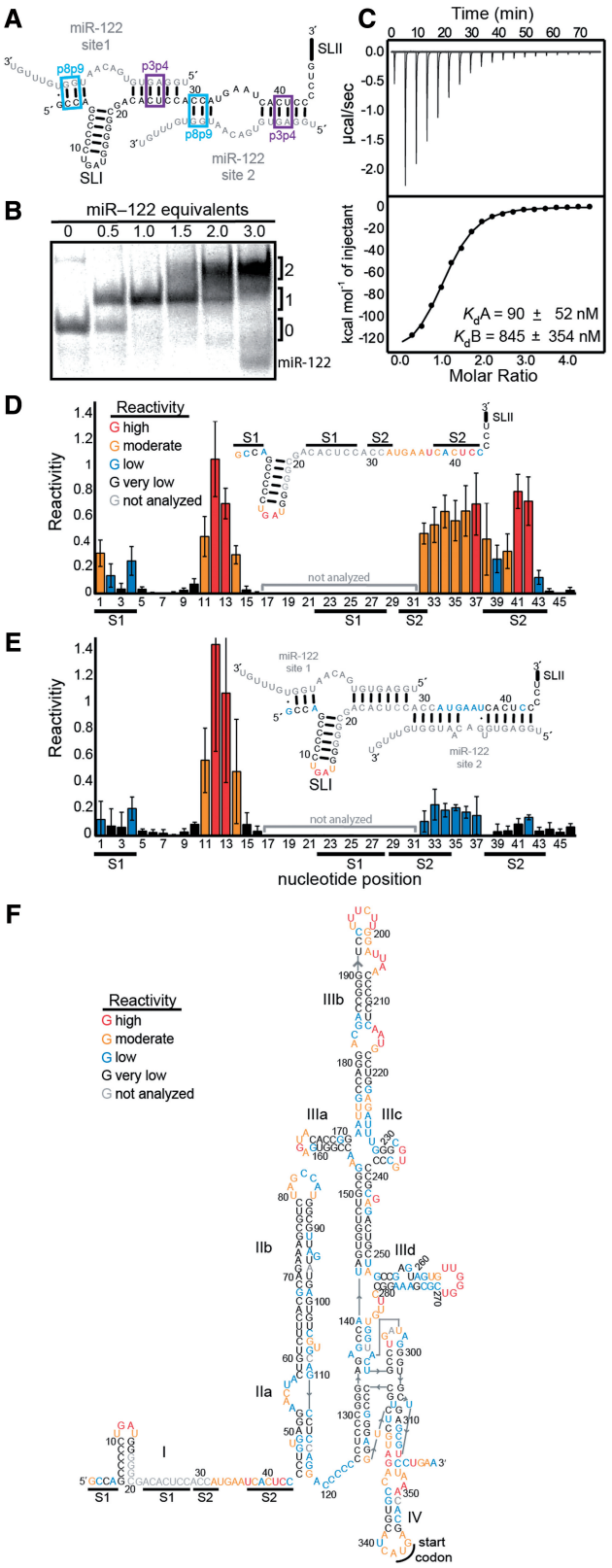

Figure 1. HCV domain I binds two copies of miR-122. (**A**) Model of the interaction of HCV dom I (black) with miR-122 (grey). (**B**) Non-denaturing gel electrophoresis mobility shift assay performed in the presence of 5 mM Mg^{2+} and increasing amounts of miR-122. (**C**) Thermogram and resulting binding curve for the titration of HCV dom I with miR-122. The dissociation constants are the mean of three replicates with error propagated from the three individual binding curve fits. (**D** and **E**) SHAPE reactivities of HCV dom I in the absence (D) and presence (E) of 10 µM miR-122. Reactivities are represented as the mean of three replicates with standard deviation shown as error bars. Reactivities are superimposed on the secondary structures according the legend in (D) with the exception of nucleotides 17–31 of dom I, which are omitted in data analysis owing to high background from a large reverse transcriptase stop in the raw electropherogram (Supplementary Figure S2A). (**F**) SHAPE reactivities superimposed on the secondary structure model of the entire HCV 5′UTR RNA colored as in (D).

HCV 5′UTR and/or genome. These results reveal a mechanism of miRNA action in post-trancriptional gene regulation that involves structural changes induced on formation of the miRNA:HCV complex.

MATERIALS AND METHODS

Synthesis of HCV 5′UTR RNA

For selective 2′-hydroxyl acylation analysed by primer extension (SHAPE) analysis, a DNA template for transcription inserted in the context of 5′ and 3′ flanking sequences (18) was prepared using PCR [1 mL; 20 mM Tris (pH 8.4), 50 mM KCl, 2.5 mM $MgCl_2$, 200 µM each NTP, 0.5 µM each forward and reverse primer, 1 µg DNA template and 0.025 U/µL of Taq polymerase; denaturation at 94°C, 45 s; annealing 60°C, 30 s; and elongation 72°C, 1 min; 34 cycles] from the plasmid pKB101, a variation of pKB84 that includes domain I (19), using the following primers: forward 5′-TAATACGACTCACTATAGGCCT TCGGGCCAAGCCAGCCCCCTGATGGGGG-3′ and reverse 5′-GAACCGGACCGAAGCCCGATTTGGTTT TTCTTTGAGGTTCAGGATTTGTGCTC-3′. For isothermal titration calorimetry (ITC) experiments, a DNA template for transcription was prepared by linearization of pKB101 with BamHI (NEB). Transcription reactions (100 µL for SHAPE, 5.0 mL for ITC, 37°C for 3–4 h) contained 30 mM Tris (pH 8.0), 25 mM $MgCl_2$, 2 mM spermidine, 0.01% (v/v) Triton X-100, 5 mM each NTP, 1 µg/mL of inorganic pyrophosphatase (Roche), 50 µg/mL of DNA template, 0.1 mg/mL of T7 RNA polymerase and 0.12 U/µL of RNase Inhibitor (Promega). The RNA for ITC was purified by denaturing polyacrylamide gel electrophoresis (8% 29:1 acrylamide:bisacrylamide, 7 M Urea), whereas the RNA for SHAPE experiments was purified using the RNA clean and concentrator-25 kit (Zymo research).

Electrophoretic mobility shift assays with HCV dom I RNA

RNA oligonucleotides corresponding to HCV dom I and native and mutant miR-122 RNAs were synthesized by Integrated DNA Technologies (IDT). HCV dom I RNA (8 µM) was heated at 65°C for 5 min and cooled to ~35°C before addition of native or mutant miR-122 RNAs in molar ratios of 0, 0.5, 1.0, 1.5, 2.0 and 3.0 and incubated at 37°C for 20–30 min in a 5 µL volume containing 100 mM HEPES (pH 7.5), 100 mM KCl and 5 mM $MgCl_2$. An equal volume of gel-loading dye (30% glycerol, 0.5× TBE and 6 mM $MgCl_2$) was added before separation using non-denaturing gel electrophoresis

(12% 29:1 acrylamide:bisacrylamide, 0.5× TBE, 6 mM $MgCl_2$) 8 W, 4°C, 2.5 h). RNA was visualized by staining with SYBR Gold (Invitrogen).

Isothermal titration calorimetry

RNA samples were folded by diluting (~100 μL of 100 μM—1 mM stock) into ~15 mL of buffer containing 100 mM HEPES (pH 7.5), 100 mM KCl and 0 or 5 mM $MgCl_2$ and heating to 65°C for 10 min and cooling on ice for 10 min. RNA samples were subsequently concentrated, washed twice with buffer and concentrated to an appropriate volume for ITC experiments. HCV RNA was present in the cell at a concentration of 5 μM for all titrations with miR-122 RNA except for the p8p9 mutant where a concentration of 10–20 μM was used to account for the lower affinity of the interaction. MiR-122 RNAs were present in the syringe at slightly greater than 10-fold molar excess except for the titration of HCV dom I RNA with native and p8p9 miR-122 RNAs and the titration of HCV 5′UTR and s2 RNA with native miR-122, in which case the miRNAS were used at a slightly greater than 20-fold molar excess to account for the possibility of 2:1 binding. ITC experiments were performed on an ITC200 (MicroCal) instrument at 37°C, with a reference power of 3 μcal/s. In a typical experiment, we performed twenty 2.0 μL injections of miR-122 into the cell containing HCV RNA, with a duration of 4.0 s per injection and 180-s spacing. Experiments were performed in triplicate for all HCV constructs. The first injection was discarded, and the data were fitted to either a single- or two-site binding model using Origin 7 (MicroCal).

SHAPE analysis

HCV 5′UTR RNA in the context of 5′ and 3′ flanking sequences (see earlier in the text) was modified with 1M7 (3.5 mM, final) as described previously (20). MiR-122 RNAs were present at a final concentration of 10 μM, with the exception of the p8p9 miR-122, which was at a concentration of 20 μM, and incubated with folded HCV 5′UTR for 20–30 min at 37°C before modification. The general procedure of primer extension and data analysis was according to that outlined elsewhere (21).

Electrophoretic mobility shift assays with HCV s1 and s2 RNAs

MiR-122 RNAs (IDT) were 5′^{32}P-labelled using [γ-^{32}P]ATP (PerkinElmer) and T4 PNK (NEB) [10 μL of reaction; 1× T4 PNK buffer, 50 pmol miR-122 RNA, 50 μCi [γ-^{32}P]ATP, 10 U T4 PNK] at 37°C for 1 h and subsequently diluted with nuclease-free water (40 μL). Excess [γ-^{32}P]ATP was removed using a G25 spin column (GE healthcare), and the resulting radio-labelled miR-122 RNAs were used without further purification. HCV s1 and s2 RNAs were folded by heating at 65°C for 5 min and cooling on ice for 5–10 min in folding buffer [5 mM $MgCl_2$, 100 mM KCl and 100 mM HEPES (pH 7.5)]. The pre-folded s1 and s2 RNAs were serial diluted by 2-fold in folding buffer to obtain desired concentration range before incubation with ~3000 cpm/μL (~0.5–1 pmol) in a 5 μL of reaction for 20–30 min at 37°C. An equal volume of gel-loading dye (30% glycerol, 0.5× TBE and 6 mM $MgCl_2$) was added before separation using non-denaturing gel electrophoresis (14% 29:1 acrylamide:bisacrylamide, 0.5× TBE, 6 mM $MgCl_2$) 8 W, 4°C, 2.5 h). RNA was visualized by phosphorimaging using a Storm840 (GE healthcare).

Xrn1 nuclease activity assays

5′phosphorylated and 3′ ^{32}P-labelled RNA substrates were prepared by labelling a synthetic RNA oligonucleotide corresponding to nucleotides 1–47 of HCV genotype 1b (IDT) with [5′-^{32}P]pCp and T4 RNA ligase (NEB) [30 μL of reaction; 1× T4 RNA ligase buffer (NEB), 1 mM ATP, 10% (v/v) DMSO; 100 pmol RNA, 1 μM [5′-^{32}P]pCp (PerkinElmer) and 10 U T4 RNA ligase] overnight at 16°C and subsequently 5′phosphorylated using T4 PNK (10 U) for 1 h at 37°C. Excess ATP and 5′-^{32}P]pCp were removed using a G25 spin column (GE Healthcare); the resulting radiolabelled RNAs were used without further purification. Assays were carried out in 1× Xrn1 buffer [20 mM HEPES (pH 7.5), 100 mM KCl, 4 mM $MgCl_2$, 5% (v/v) glycerol, 1 mM DTT] with 1 μg of hXrn1 and ~2 pmol RNA substrate at 25°C for 1 min to 3 h. Reactions were quenched by addition of an equal volume of RNA-loading dye [95% (v/v) deionized formamide, 5 mM ethylenediaminetetraacetic acid (pH 8.0), 0.025% (w/v) sodium dodecyl sulphate]. Native and mutant miRNAs (10 μM, final) were incubated for 30 min at 25°C with labelled RNA substrate before addition of Xrn1. The reaction products were resolved by running the samples on a 16% polyacrylamide/7 M urea gel.

RNA stability in HepG2 lysate

HepG2 lysate was prepared according to standard protocols (22). 5′phosphorylated and 3′ ^{32}P-labelled RNA substrates prepared as in Xrn1 assays were incubated in HepG2 lysate at 25°C for 0.01–3 h in the presence of 5 mM $MgCl_2$, 100 mM KCl and 100 mM HEPES (pH 7.5). The assay was performed identically to the Xrn1 activity assay except in the case of 5′phosphorylated miR-122, which was incubated with extract before addition of RNA substrate to allow for loading into Ago2.

RESULTS AND DISCUSSION

MiR-122 binds at two non-equivalent sites in the HCV 5′ UTR

Two distinct binding sites for miR-122 were previously identified within the HCV 5′UTR based on sequence conservation and compensatory base-pairing mutations (8,9). However, whether HCV forms a stable complex with two copies of miR-122 simultaneously was not known. To test this possibility, we incubated an RNA derived from the HCV genotype 1b consisting of both predicted miR-122 binding sites with increasing concentrations of miR-122. The resulting miR-122:HCV complexes were resolved by non-denaturing gel electrophoresis (Figure 1B). The HCV transcript showed a retarded mobility on addition of one molar equivalent of miR-122, and this complex was

Table 1. ITC analysis of miR-122 binding by HCV 5′UTR RNA constructs

HCV RNA (nt)		Site 1 (1–30)	Site 2 (21–47)	Dom I (1–47)		5′ UTR (1–371)	
miR-122 RNA	Mg^{2+} (mM)	K_d (nM)[a]	K_d	K_ds1	K_ds2	K_ds1	K_ds2
Native	5	14 ± 6.2	13 ± 9.6	845 ± 354	90 ± 52	11 600 ± 9400	208 ± 80
p3p4	5	n.b.	35 ± 8.8	n.b.	120 ± 25	n.b.	32 ± 9.2[b]
p8p9	5	+	235 ± 133[b]	+	2306 ± 1041	+	+
Native	0	n.b.	72 ± 14	n.b.	130 ± 33	n.b.	19 ± 6.3[b]

[a]Values reported are means of three measurements ± error propagated from individual fits.
[b]Values reported are means of two measurements.
n.b. = no binding observed; + = binding observed but K_d not determined.

further retarded on addition of two molar equivalents of miR-122, indicating formation of a stable trimeric complex. No further mobility shift occurred with additional miR-122, and excess miR-122 was observed as a faster migrating band in the gel under these conditions. These data show that a stable tri-molecular complex forms between the HCV 5′UTR and two copies of miR-122.

We next tested the affinities of the two miR-122 RNAs for their binding sites in the HCV RNA. Although the location and extent of base pairing is predicted to be similar for sites 1 and 2 (Figure 1A), based on current models, there is potential for overlap in base pairing between the two sites, which could lead to unequal affinities and competition for binding. Binding affinities for the interaction between HCV domain I (dom I, nucleotides 1–47) and miR-122 RNA were measured using ITC. Using established conditions, miR-122 was titrated into a solution of pre-annealed HCV dom I RNA, resulting in a strongly exothermic interaction ($\Delta H = -141$ kcal/mol) indicating an enthalpically favourable interaction (Figure 1C, top panel and Supplementary Table S1). The binding curve was best fit with a two-site binding model, yielding equilibrium dissociation constants (K_ds) of 90 ($n = 0.94$) and 845 nM ($n = 0.94$) (Figure 1C, bottom panel and Table 1). This result indicates that miR-122 has different affinities for site 1 compared with site 2 in the HCV 5′ UTR. In liver cells, where the concentration of miR-122 is likely to be in the low nM range (~66 000 copies/cell) (4), these two partially overlapping miR-122 binding sites may compete for occupancy. ITC was also performed on the interaction between miR-122 and dom I in the context of the full-length HCV 5′UTR [dom I + internal ribosome entry site (IRES), nucleotides 1–371], with a result in overall agreement with that for the HCV dom I RNA alone (Supplementary Figure S1A, Table 1 and Supplementary Table S1).

To investigate the molecular origin of the distinct affinities for the two binding sites in dom I, we performed SHAPE (20) on the full-length HCV 5′UTR (nucleotides 1–371) in the presence and absence of miR-122 RNA (Figures 1D–F and 2 and Supplementary Figures S2 and S3). SHAPE provides nucleotide resolution information on local nucleotide flexibility and provides structural information for each nucleotide in the RNA sequence (23). When SHAPE was performed on the HCV 5′UTR alone, reactivity information was obtained for almost every nucleotide in the RNA (Supplementary Figure S2A) and agrees well with the current structural model (24,25) (Figure 1F). The reactivities observed for dom I reveal that site 2 is unstructured, and although most of the structural details for site 1 are obscured (Supplementary Figure S2A), the extreme 5′ end is also relatively unstructured (Figure 1D). When SHAPE was performed on the HCV 5′UTR in the presence of miR-122, reactivities indicated that the RNA folds into a similar structure outside of dom I (Figure 2 and Supplementary Figure S3). Within dom I, however, a large decrease in reactivity was observed in site 2 (Figures 1E and 2). When the dom I reactivities are superimposed on the RNA secondary structure, it is apparent that the extent of base pairing at site 2 is greater than originally proposed (Figure 1A). These results support a base-pairing pattern similar to a recent model (25), which would increase the stability of the interaction of miR-122 at site 2 compared with site 1 (Figure 1E). We also observed a reproducible decrease in reactivity at the extreme 5′ end of the HCV RNA, consistent with miR-122 binding at site 1. Other reproducible differences in reactivity occur outside of dom I on miR-122 binding, mostly within the pseudoknot and dom IV regions, this agrees with what has been observed in other similar experiments and is an intriguing result (25). There is also a prominent increase in reactivity within the bulged region in dom IIa (Figure 2). Notably, dom IIa and IIb has also been observed to have increased SHAPE reactivity and hence flexibility in the absence of dom I [see Supplementary Figure S6b in (24)]. Interestingly, the dom IIa bulge is the binding site of an inhibitor of viral translation and affects the dynamics and tertiary structure in dom II (26). These SHAPE-reactivity changes could result from changes in the global tertiary structure that arise on binding of miR-122 to dom I, including possible stacking interactions between the two duplexes that form as a result of binding and/or disruption of an interaction between dom I and IIa. These results are intriguing, but further work needs to be done to address these possibilities entirely and in greater detail. Dom I is located immediately adjacent to the HCV IRES, which comprises the rest of the 5′UTR and is necessary for viral translation. Although evidence for modest miR-122-mediated stimulation of HCV translation is controversial (27,28), binding of miR-122 to dom I could affect the interaction of this domain with the HCV

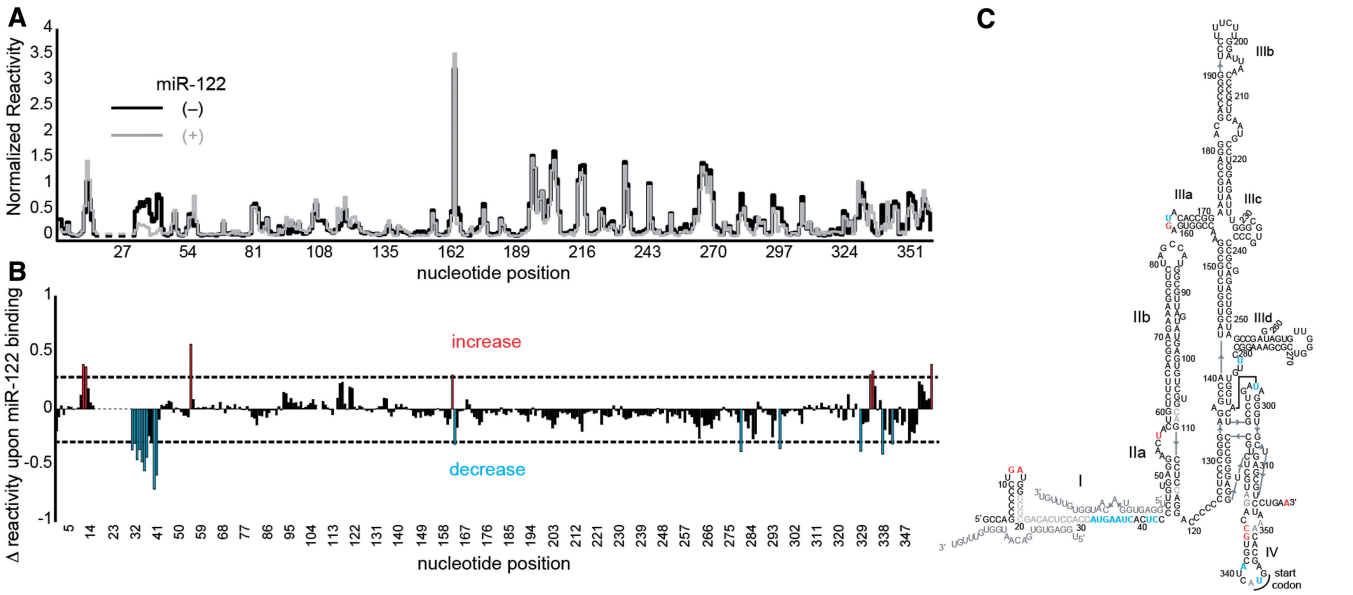

Figure 2. Observed changes in reactivity upon miR-122 binding to the full length HCV 5′UTR. (**A**) Step plot comparing quantified and normalized SHAPE reactivities obtained in the absence (black line) or presence (grey line) of native miR-122. (**B**) Difference plot showing changes in reactivity on binding of miR-122. Significant increases in reactivity (more than Δ0.3 SHAPE units) are highlighted in red, whereas substantial decreases in reactivities (more than −Δ0.3 SHAPE units) are shown in blue. (**C**) Changes in reactivity on binding of miR-122 superimposed on the proposed secondary structure of the HCV 5′UTR coloured as in (B).

IRES and hence influence viral translation by altering the global structure of this region. Although we do not observe enhanced binding affinity of the HCV IRES to the 40S ribosomal subunit in the presence of miR-122 (S.A.M and J.A.D. unpublished results), miR-122 binding could have a kinetic effect on translation initiation or trigger a more complex chain of events in other aspects of the viral RNA life cycle.

HCV domain I interacts with miR-122 using extensive base pairing outside the seed region

Most miRNA:target interactions are sensitive to mutations in the base pairs within the canonical seed sequence consisting of nucleotides 2–8 of the miRNA (12). In agreement with this finding, mutation of base pairs 3 and 4 (p3p4, Figure 1A) is detrimental to miR-122 function in HCV RNA upregulation when directed at both site 1 and site 2 (2,8). We wanted to test the contribution of these seed-sequence base pairs, as well as that from base pairs that form downstream of the canonical seed sequence (p8p9, Figure 1A), to the stability of the miR-122:HCV complex. We first assessed the ability of the mutated miR-122 RNAs, p3p4 and p8p9, to form a stable complex with HCV dom I RNA using an electrophoretic mobility shift assay. When HCV dom I was incubated with increasing molar equivalents of p3p4 miR-122 and resolved on a non-denaturing polyacrylamide gel, a single slower-migrating species was detected (Figure 3A, left hand lanes). When HCV dom I was incubated with the p8p9 miR-122, two slower-migrating species were observed as with the native miR-122 sequence, although the poor resolution of the complex suggests that it is less stable compared with the native complex (compare right hand lanes in Figure 3A with Figure 1B). These data indicate that both the seed region and downstream base pairing are important to the stability of this miRNA:target interaction.

To more quantitatively assess the contribution of each base-pairing region to the stability of the complex, ITC was performed using the p3p4 and p8p9 miR-122 mutated sequences. When p3p4 miR-122 was titrated into folded HCV dom I, the resulting thermogram revealed a strongly exothermic binding interaction ($\Delta H = -118$ kcal/mol, Supplementary Table S1) with a resulting 1:1 binding curve ($n = 0.94$) and a K_d of 120 nM (Figure 3B, left panel). Although only one copy of the mutated miR-122 binds, it binds with similar affinity to the native miR-122 sequence (Table 1, <2-fold difference). The thermogram produced from the titration of p8p9 miR-122 mutation into HCV dom I was less exothermic ($\Delta H = -26.5$ kcal/mol, Supplementary Table S1) and again resulted in an approximate 1:1 binding curve ($n = 0.67$) but with a much weaker K_d of 2.3 μM (Figure 3B, right panel). Binding of a second miR-122 is not observed, even though a ratio of almost 5:1 miR-122:HCV dom I was reached during the course of the titration, suggesting the K_d is weaker than can be measured by ITC (see 'Materials and Methods' section). The affinity of the p8p9 miR-122 for HCV dom I is significantly lower than that of both the p3p4 and native miR-122 sequences (~19 and ~26-fold, respectively), indicating that those base pairs contribute greatly to the overall stability of the miRNA:target interaction. This result is in contrast to what has been observed for canonical miRNA:target interactions, where downstream base pairing is not as vital to miRNA function and binding stability (12). Furthermore, these results show that the two miR-122 binding sites behave differently.

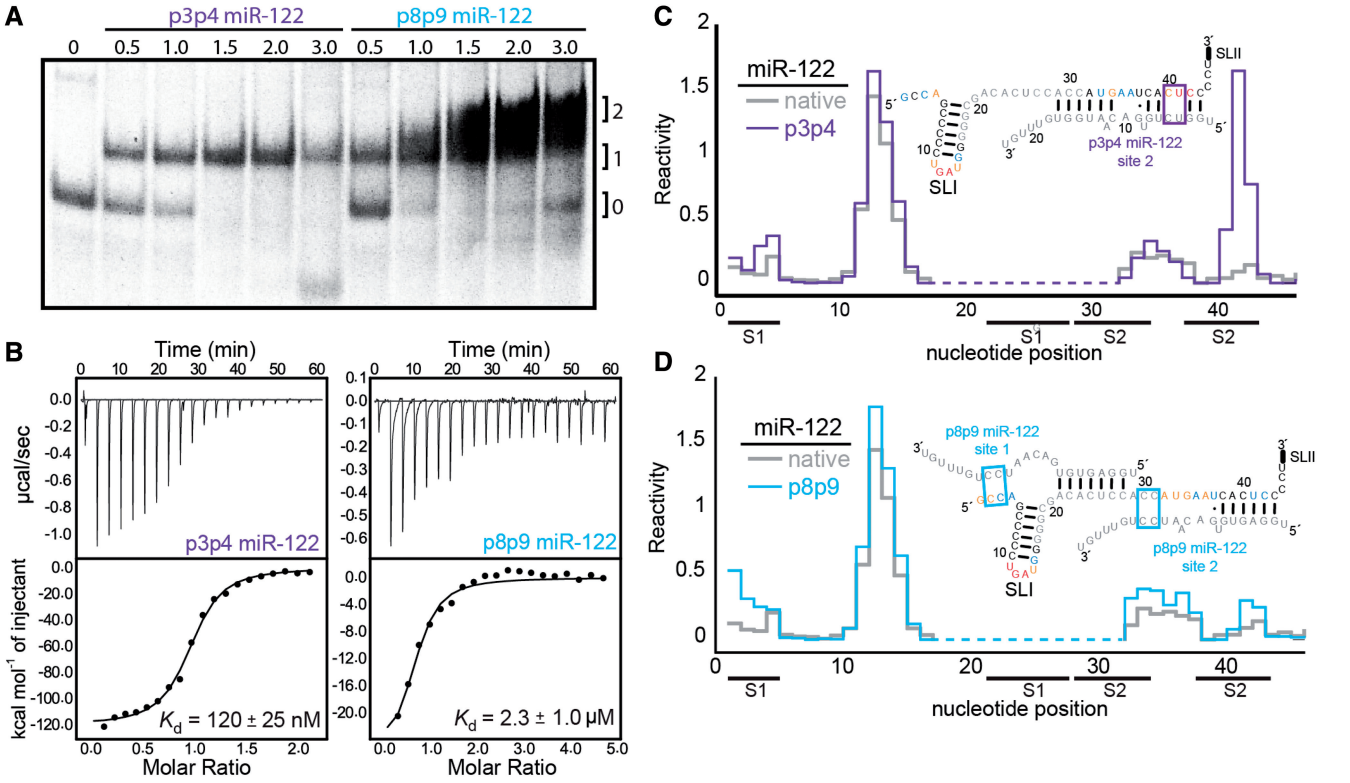

Figure 3. The interaction between HCV dom I and miR-122 is sensitive to mutations within and downstream of the seed sequence. (**A**) Electrophoretic mobility shift assay with mutated miR-122 sequences. The p3p4 miR-122 contains seed sequence mutations (left panel) and the p8p9 miR-122 contains downstream base pairing mutations (right panel). No slower migrating species were observed at concentrations of the p3p4 mutant higher than two molar equivalents relative to the HCV RNA. (**B**) Thermograms and resulting binding curves for the titration of HCV dom I with p3p4 (left) and p8p9 (right) miR-122 RNA mutants. (**C** and **D**) SHAPE reactivities of HCV dom I in the presence of 10 μM p3p4 miR-122 (C, purple outline) or 20 μM p8p9 miR-122 (D, cyan outline) compared with native miR-122 (grey outline). Reactivities shown are the mean of three replicates and are superimposed on the secondary structures according the legend in Figure 1D.

At one site, the contribution of binding energy from the seed sequence is imperative to the overall stability of the interaction, whereas at the other site, the seed sequence pairing contributes only marginally to the overall interaction stability. These results further support the conclusion that miR-122 has much higher affinity for one site versus the other.

HCV domain 1 site 2 is the high affinity site for miR-122 owing to extensive base pairing outside the seed sequence

As the two sites display different behaviour with respect to their interaction with miR-122, despite somewhat similar sequences, we designed RNAs that represent site 1 and site 2 (named s1 and s2, respectively) independently to determine which is the high-affinity site (Figure 4A). To examine how these two sets of RNAs bind the native miR-122 sequence, we performed both electrophoretic mobility shift assays with ^{32}P-labelled miR-122 (Figure 4B) and ITC experiments (Supplementary Figure S4). Both s1 and s2 RNAs are capable of binding miR-122 with nearly identical K_d values of 14 and 13 nM, respectively (Table 1). These findings contrast with the affinities measured when the two sites are juxtaposed in the context of dom I, indicating the two sites compete for binding with miR-122 and are therefore partially overlapping. Strikingly, when the same mobility shift assay is performed using p3p4 miR-122, no binding is observed with up to μM amounts of s1 RNA, whereas binding to s2 is observed in the low nM range (Figure 4C). These results support the notion that miR-122 has very different affinities for the two binding sites within the HCV 5′UTR. Interestingly, site 1 resembles a canonical miRNA:target site based on the necessity of a seed sequence in the interaction, whereas the same mutations in the site 2 seed sequence contribute little to the overall binding energy and stability of the interaction. HCV s1 and s2 RNAs are both capable of binding ^{32}P-labelled p8p9 miR-122, albeit much more weakly compared with native miR-122 (Supplementary Figure S4). The fact that s1 RNA can still bind the p8p9 mutated miR-122, but not the p3p4 mutated miR-122, is reminiscent of a more conventional miRNA:target interaction, with the seed sequence contributing more to the interaction compared with any downstream base pairing that occurs. Conversely, in site 2, downstream base pairing is much more important for the stability of the miRNA:HCV interaction compared with the seed sequence. This is an unanticipated result in light of our current understanding of miRNA:target interactions.

We then performed SHAPE on the HCV 5′UTR in the presence of both the p3p4 and p8p9 miR-122 RNAs to investigate the structural impact of binding by these

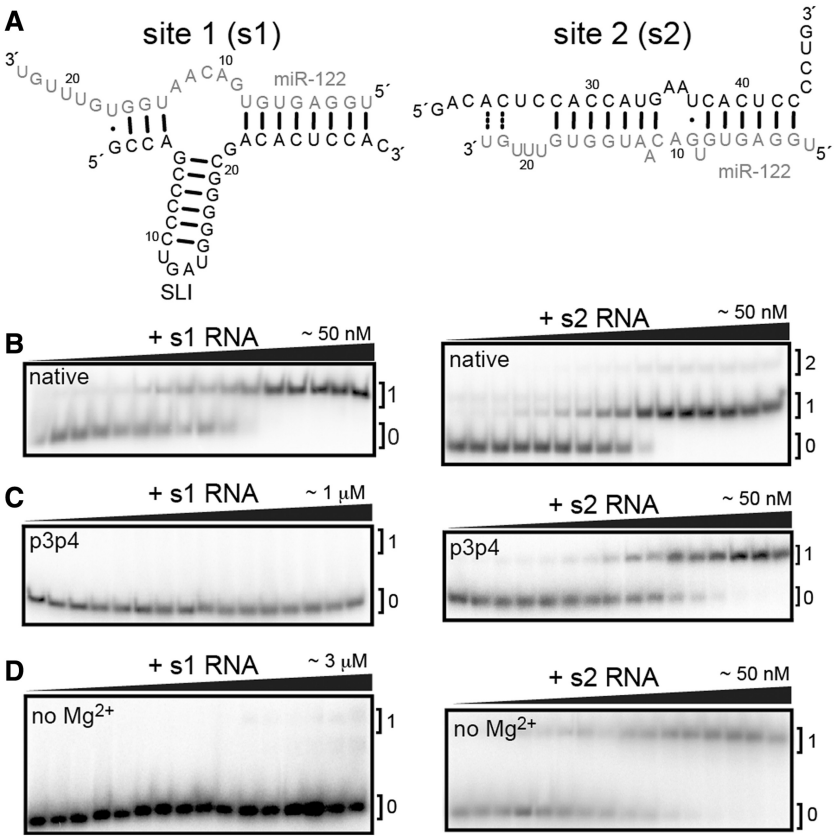

Figure 4. Determination of site 1 and site 2 interactions with miR-122 RNAs. (**A**) Proposed base-pairing interactions of each site individually with miR-122. The sequence of the site 1 (s1) and site 2 (s2) RNAs are meant to represent binding to miR-122 independently. The s2 RNA is capable of weak binding to a second copy of miR-122 owing to the presence of the s1 seed sequence (nucleotides 22–29) within the s2 RNA. Electrophoretic mobility shift assays of s1 and s2 RNAs with ^{32}P-labelled native (**B**) and p3p4 (**C**) miR-122 and (**D**) in the absence of Mg^{2+} ions.

mutated sequences. Overall, the reactivity pattern for the 5′UTR in the presence of each mutated miR-122 RNAs is similar to that observed for the native sequence (Supplementary Figure S5A and B). Careful inspection of the dom I reactivities in the presence of p3p4 miR-122 reveals a large increase in reactivity at nucleotides 40–42 and a small but reproducible increase in reactivity at nucleotides 1–4 (Figure 3C). The rest of the base pairing at site 2 is seemingly undisturbed by this local mutation and is consistent with the overall similar binding behaviour compared with that of native miR-122 RNA. The reactivity increase at nucleotides 1–4 is consistent with a lack of binding of the p3p4 miR-122 at this site (Figure 3C). Overall, the reactivities of dom I increase in the presence of p8p9 miR-122 compared with native miR-122 (Figure 1D). The seed sequence complement of site 2 remains mostly unreactive, whereas the downstream sequence becomes moderately reactive. This suggests a much less stable interaction in which the base pairs outside the seed sequence are incompletely or transiently formed, which explains the lower affinity observed for site 2 via gel shift and ITC experiments. Similarly, the reactivities at nucleotides 1–4 are increased in the presence of p8p9, indicating loss of the downstream base pairing at site 1.

These results suggest that both the seed sequence and downstream pairing are important contributors to the overall stability and hence to the function of the interaction of miR-122 with HCV RNA. Surprisingly, the contribution of seed sequence and downstream base pairing is not equivalent in the two sites. Site 1 behaves similarly to a canonical miRNA:target interaction, whereas site 2 forms an unconventional and high-affinity interaction with a miRNA, driven by extensive base pairing outside of the canonical seed sequence interaction. As a stable tri-molecular complex forms between two potentially overlapping copies of miR-122 and HCV transcripts with extensive base pairing, the question of whether any higher-order interactions contribute to the stability of the complex still remains.

The miR-122:HCV complex comprises higher-order interactions

As a step towards understanding whether tertiary interactions play an important role in forming this unconventional miRNA:target interaction, we tested the ability of miR-122 to bind HCV dom I RNA in the absence of magnesium ions. Withholding Mg^{2+} prevents the formation of RNA tertiary structures and therefore may alter the accessibility of the RNA structures. We incubated HCV dom I RNA with increasing molar amounts of miR-122 RNA in the absence of Mg^{2+}. When we resolved the resulting complexes using non-denaturing poly-acrylamide

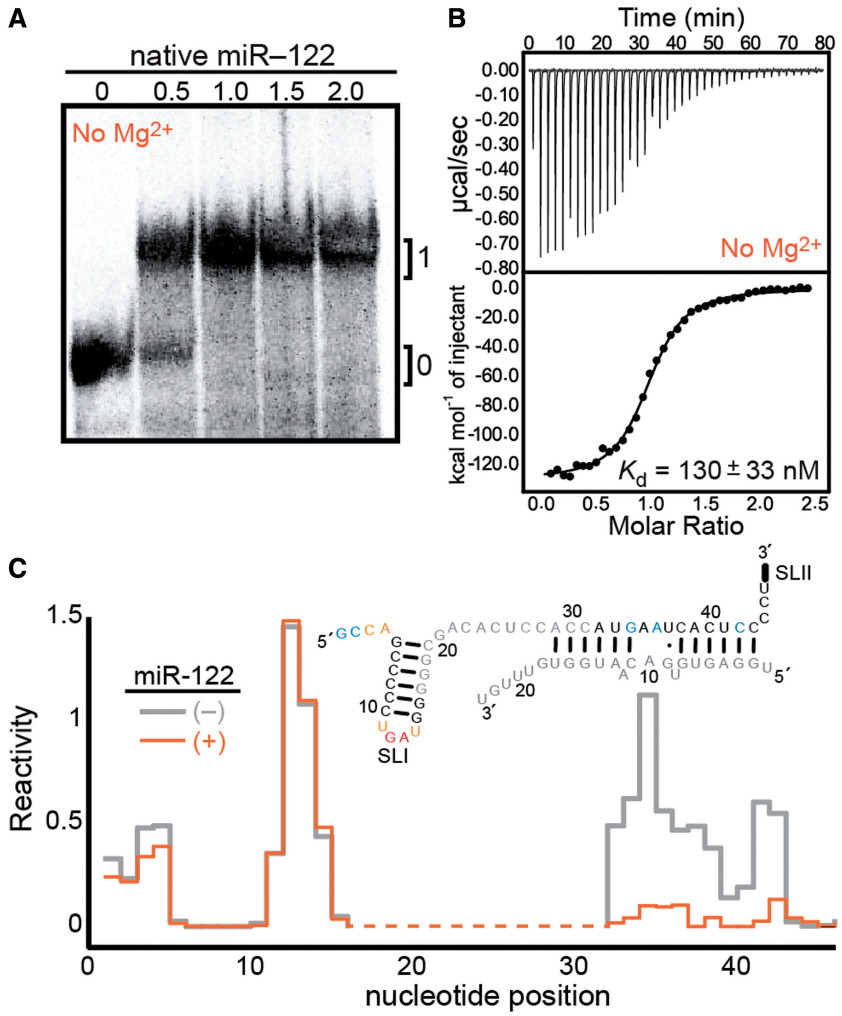

Figure 5. The interaction between HCV dom I and miR-122 requires Mg^{2+} ions. (**A**) Electrophoretic mobility shift assay with HCV dom I and increasing amounts of miR-122 performed in the absence of magnesium. (**B**) Thermogram and resulting binding curve of the titration of HCV dom I with native miR-122 in the absence of Mg^{2+} ions. (**C**) SHAPE reactivities of HCV dom I folded in the absence of magnesium and with (orange outline) or without (grey outline) 10 µM miR-122. Reactivities shown are the mean of three replicates and are superimposed on the secondary structures according the legend in Figure 1D.

gel electrophoresis, we observed one copy of miR-122 bound stably to HCV dom I but did not observe a slower migrating complex beyond a 1:1 ratio of miR-122:HCV (Figure 5A). This result indicates that formation of the native complex is severely hindered and that a higher-order structure may be formed that requires stabilization by Mg^{2+}. We quantified the affinity for miR-122 to HCV dom I in the absence of Mg^{2+} using ITC. When HCV dom I is titrated with miR-122 in the absence of Mg^{2+}, the resulting thermogram is strongly exothermic ($\Delta H = -130$ kcal/mol, Supplementary Table S1) with a binding curve best fit to a 1:1 binding model ($n = 0.999$) with a K_d of 130 nM (Figure 4B). The affinity of miR-122 for HCV in the absence of Mg^{2+} is only 1.4-fold weaker compared with the affinity of native miR-122 for site 2 when Mg^{2+} is present (Table 1). When we performed the same experiment in the context of the entire HCV 5′UTR, we obtained a similar result (Table 1 and Supplementary Figure S1C). To conclusively determine which miR-122 binding site is impaired in the absence of Mg^{2+}, we performed electrophoretic mobility shift assays with ^{32}P-labelled native miR-122 RNA and the s1 and s2 RNAs. No significant binding was observed with s1 RNA up to concentrations of 3 µM. Conversely, when s2 was added, binding was observed in the low nM range (Figure 4D). This result supports the notion that site 2 is the more stable site, and that formation of the fully functional trimeric complex between miR-122 and HCV RNA requires Mg^{2+} to stabilize higher-order interactions within the complex.

We also investigated Mg^{2+}-induced structural changes in the HCV 5′UTR in the absence and presence of miR-122. To do this, we performed SHAPE with and without miR-122 in the absence of Mg^{2+}. Overall, the reactivity pattern of the HCV 5′UTR in the presence and absence of miR-122 when Mg^{2+} is absent is similar (Supplementary Figure S5C). Inspection of the reactivities for dom I reveals that site 2 is bound by miR-122, as evident from the substantial decrease in reactivities of nucleotides 32–43. The reactivities for nucleotides 1–4

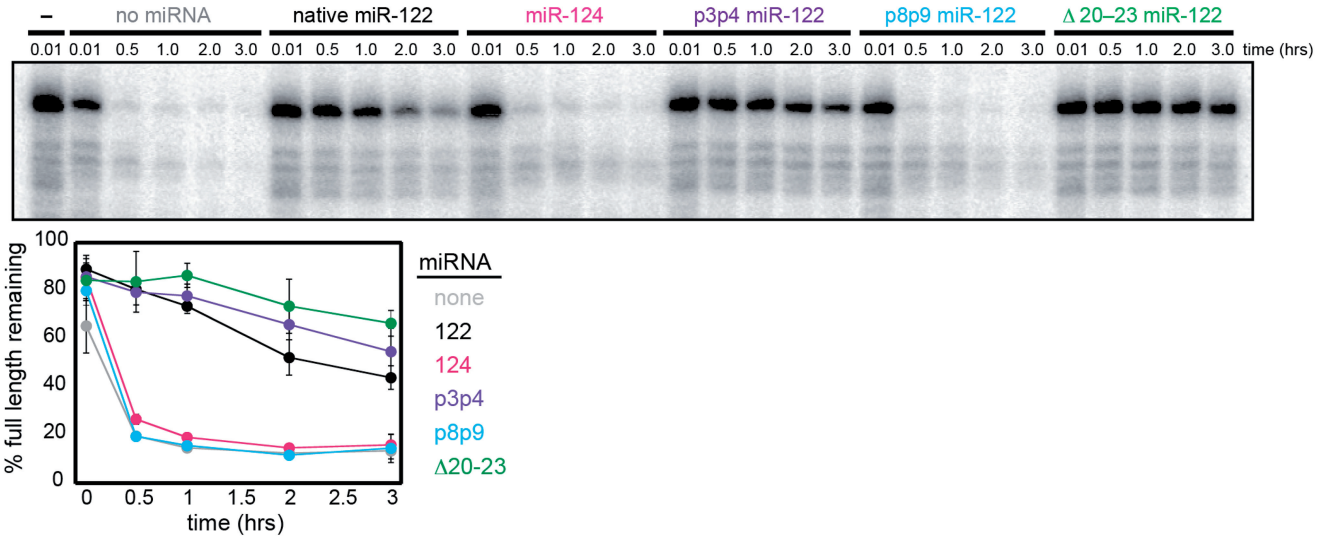

Figure 6. Susceptibility of 5′ monophosphorylated HCV dom I to Xrn1-mediated degradation in the presence of miR-122. Stability of 5′ monophosphorylated 3′-^{32}P-labelled HCV dom I RNA after incubation with Xrn1 in either the absence or presence of native and mutant miR-122 RNAs for a period of minutes to 3 h resolved by denaturing gel electrophoresis (top). The percentages of full-length RNA remaining (below) are shown as the average of two independent experiments with standard deviation shown as error bars with values normalized to the no-Xrn1 control.

remain moderate even in the presence of miR-122, indicating that no miR-122 is bound at site 1.

Performing the SHAPE experiment on the entire HCV 5′UTR reveals Mg^{2+}-induced structural changes throughout the entire RNA and allows the exploration of possible tertiary interactions. When we compare the reactivities for the HCV 5′UTR in the absence or presence of Mg^{2+}, the overall pattern is similar, indicating that the secondary structure has not been dramatically altered. However, there are several regions with large reproducible changes in reactivity, indicating local changes in tertiary structure (Supplementary Figure S6). Interestingly, there are several increases in reactivity in dom I on the removal of Mg^{2+}, likely indicating long-range interactions between this domain and other parts of the 5′UTR, with potential implications for the binding and regulation by miR-122. There are also increases in reactivity in dom IIb, which is a reasonable candidate interaction partner for dom I. Notably, dom II has a bent L-shape architecture (29), and it is anticipated that these domains are spatially adjacent based on observations made in the context of the HCV IRES bound to the 40S or 80S ribosomes (30,31). Other Mg^{2+}-induced changes in reactivity are seen throughout dom III, indicating additional possible tertiary interactions with potential implications in 40S and translation initiation factor eIF3 binding and hence translation of the viral RNA.

The miR122:HCV interaction imparts stability by protection from an exonuclease

The mechanism by which miR-122 augments HCV RNA stability and infectivity remains unknown, but recent reports have suggested that it may shield the 5′ end of the viral RNA from degradation by cytosolic RNA exonucleases (5,9,10). The 5′ end of HCV RNA from HCV replicon-containing cells is modified with a single phosphate, rendering it a potential substrate for the primary eukaryotic cytosolic 5′→3′ RNA exonuclease Xrn1 (32,33). We wondered whether the stable complex detected at the HCV 5′ end in the presence of miR-122 (25) functions as a steric block to Xrn1-catalyzed nucleolytic degradation. To investigate this possibility, we first tested whether HCV dom I on its own is a substrate for human Xrn1 *in vitro*. Our results show that 5′ monophosphorylated HCV is subject to degradation by Xrn1 in the absence of miR-122 (Supplementary Figure S7). Furthermore, prior incubation with miR-122 can prevent degradation of HCV dom I by Xrn1 (Supplementary Figure S7).

We reasoned that if protection from Xrn1 is the primary function of miR-122 in stabilizing HCV RNA, then mutations that are detrimental to miR-122 function *in vivo* should not protect HCV RNA from Xrn1-mediated degradation. To test this idea, we used three miR-122 mutants that are defective in supporting HCV RNA levels in a replicon system (8,9). Two of these mutants, p3p4 and p8p9 described in this study, contain point mutations that disrupt HCV 5′UTR complex formation, whereas the third mutant, Δ20–23, lacks the last four 3′ nucleotides of the native miR-122 sequence yet forms a complex with the HCV 5′UTR (Supplementary Figure S8) (9). When HCV dom I was incubated with these mutated miR-122 RNAs under conditions that support complex formation with wild-type miR-122, both p3p4 and Δ20–23 protected the HCV RNA from subsequent Xrn1-mediated degradation. In contrast, neither p8p9 nor the unrelated miRNA miR-124 provided protection from Xrn1-mediated degradation (Figure 6). These results suggest that the ability of miR-122 to promote HCV infectivity is independent of its capacity to protect the viral RNA from Xrn1. The ternary complex formed between the HCV 5′UTR and

miR-122 must play additional or alternative roles *in vivo*, perhaps through interactions with other cellular factors. It could be that the affinities of the miR122-RISC complex to the HCV RNA in cells differ from those measured by our *in vitro* system using naked RNA. These differences in affinities could explain the inconsistent results with Xrn1; however, while this article was under revision, another study using cell-based assays reported to observe that miR-122 protects HCV RNA from 5′decay, yet Xrn1 knockdown does not rescue replication of a viral mutant defective in miR-122 binding (34). The conclusion of the study was that miR-122 has additional functions in the viral life cycle and is in strong agreement with the results obtained with our reconstituted *in vitro* system.

A unique miRNA:target interaction contributes to an unconventional function

To explore the possibility that other cytosolic exonuclease(s) act on the HCV RNA 5′ end, we tested the stability of HCV RNA in HepG2 cell lysate in the presence and absence of native and mutant miR-122 RNAs. Both the wild-type miR-122 and the p3p4 and Δ20–23 mutant miR-122 RNAs were observed to stabilize the HCV RNA at early time points in HepG2 lysate, compared with HCV RNA incubated in lysate in the presence of the unrelated miR-124 or in the absence of miRNA (Supplementary Figure S9). We also pre-incubated miR-122 with the HepG2 cell lysate to allow for loading into Ago2, accounting for the possibility that it is absolutely required for stabilization, which has been done previously (10). Despite pre-incubation, we saw no enhanced stabilization of the HCV RNA (Supplementary Figure S9). These observations support the conclusion that protection from nucleolytic degradation is not sufficient to explain the role of miR-122:HCV RNA complex formation in positively regulating HCV RNA levels. A possible alternative function for miR-122 in forming this stable tri-molecular complex on the 5′ end of HCV is the recruitment of other protein factors, either directly or through an Argonaute protein, that can increase infectivity by promoting viral RNA production, translation or packaging.

Some published data support the enhanced translation of HCV RNA on miR-122 binding, although the mechanism is unclear (27,35,36). Our data suggest a possible role for miR-122 in affecting the global architecture and dynamics of the HCV IRES, which could in turn affect the kinetics and thermodynamics of translation initiation. Future work will be necessary to test this possibility as well as other functions of the stable tandem miR-122:HCV 5′ end beyond protection of viral RNA from degradation.

SUPPLEMENTARY DATA

Supplemental Data are available at NAR Online: Supplementary Table 1 and Supplementary Figures 1–9.

ACKNOWLEDGEMENTS

The authors thank Peter Sarnow, Erica Machlin and Selena Sagan for sharing and discussing their model of the miR-122:HCV interaction before its publication; Martin Jinek for providing purified human Xrn1; Ross Wilson for in depth discussions on the project and assistance with ITC; and members of the Doudna laboratory for critical reading of the manuscript.

FUNDING

National Institutes of Health (in part to J.A.D.). S.A.M. is a fellow of the Leukemia and Lymphoma Society. J.A.D. is a Howard Hughes Medical Institute Investigator. Funding for open access charge: HHMI.

Conflict of interest statement. None declared.

REFERENCES

1. Tellinghuisen,T.L., Evans,M.J., Hahn von,T., You,S. and Rice,C.M. (2007) Studying hepatitis C virus: making the best of a bad virus. *J. Virol.*, **81**, 8853–8867.
2. Jopling,C.L., Yi,M., Lancaster,A.M., Lemon,S.M. and Sarnow,P. (2005) Modulation of hepatitis C virus RNA abundance by a liver-specific MicroRNA. *Science*, **309**, 1577–1581.
3. Randall,G., Panis,M., Cooper,J.D., Tellinghuisen,T.L., Sukhodolets,K.E., Pfeffer,S., Landthaler,M., Landgraf,P., Kan,S., Lindenbach,B.D. *et al.* (2007) Cellular cofactors affecting hepatitis C virus infection and replication. *Proc. Natl Acad. Sci. USA*, **104**, 12884–12889.
4. Chang,J., Nicolas,E., Marks,D., Sander,C., Lerro,A., Buendia,M.A., Xu,C., Mason,W.S., Moloshok,T., Bort,R. *et al.* (2004) miR-122, a mammalian liver-specific microRNA, is processed from hcr mRNA and may downregulate the high affinity cationic amino acid transporter CAT-1. *RNA Biol.*, **1**, 106–113.
5. Shimakami,T., Yamane,D., Jangra,R.K., Kempf,B.J., Spaniel,C., Barton,D.J. and Lemon,S.M. (2012) Stabilization of hepatitis C virus RNA by an Ago2-miR-122 complex. *Proc. Natl Acad. Sci. USA*, **109**, 941–946.
6. Fusco,D.N. and Chung,R.T. (2011) Novel therapies for hepatitis c: insights from the structure of the virus. *Annu. Rev. Med.*, **63**, 373–387.
7. Lanford,R.E., Hildebrandt-Eriksen,E.S., Petri,A., Persson,R., Lindow,M., Munk,M.E., Kauppinen,S. and Ørum,H. (2010) Therapeutic silencing of microRNA-122 in primates with chronic hepatitis C virus infection. *Science*, **327**, 198–201.
8. Jopling,C.L., Schütz,S. and Sarnow,P. (2008) Position-dependent function for a tandem microRNA miR-122-binding site located in the hepatitis C virus RNA genome. *Cell Host Microbe*, **4**, 77–85.
9. Machlin,E.S., Sarnow,P. and Sagan,S.M. (2011) Masking the 5' terminal nucleotides of the hepatitis C virus genome by an unconventional microRNA-target RNA complex. *Proc. Natl Acad. Sci. USA*, **108**, 3193–3198.
10. Shimakami,T., Yamane,D., Welsch,C., Hensley,L., Jangra,R.K. and Lemon,S.M. (2012) Base pairing between hepatitis C virus RNA and microRNA 122 3' of its seed sequence is essential for genome stabilization and production of infectious virus. *J. Virol.*, **86**, 7372–7383.
11. Fabian,M.R. and Sonenberg,N. (2012) The mechanics of miRNA-mediated gene silencing: a look under the hood of miRISC. *Nat. Struct. Mol. Biol.*, **19**, 586–593.
12. Bartel,D.P. (2009) MicroRNAs: target recognition and regulatory functions. *Cell*, **136**, 215–233.
13. Krützfeldt,J., Rajewsky,N., Braich,R., Rajeev,K.G., Tuschl,T., Manoharan,M. and Stoffel,M. (2005) Silencing of microRNAs in vivo with 'antagomirs'. *Nature*, **438**, 685–689.

14. Elmén,J., Lindow,M., Schütz,S., Lawrence,M., Petri,A., Obad,S., Lindholm,M., Hedtjärn,M., Hansen,H.F., Berger,U. *et al.* (2008) LNA-mediated microRNA silencing in non-human primates. *Nature*, **452**, 896–899.
15. Esau,C., Davis,S., Murray,S.F., Yu,X.X., Pandey,S.K., Pear,M., Watts,L., Booten,S.L., Graham,M., McKay,R. *et al.* (2006) miR-122 regulation of lipid metabolism revealed by in vivo antisense targeting. *Cell Metab.*, **3**, 87–98.
16. Norman,K.L. and Sarnow,P. (2010) Modulation of hepatitis C virus RNA abundance and the isoprenoid biosynthesis pathway by microRNA miR-122 involves distinct mechanisms. *J. Virol.*, **84**, 666–670.
17. Berezhna,S.Y., Supekova,L., Sever,M.J., Schultz,P.G. and Deniz,A.A. (2011) Dual regulation of hepatitis C viral RNA by cellular RNAi requires partitioning of Ago2 to lipid droplets and P-bodies. *RNA*, **17**, 1831–1845.
18. Merino,E.J., Wilkinson,K.A., Coughlan,J.L. and Weeks,K.M. (2005) RNA structure analysis at single nucleotide resolution by selective 2'-hydroxyl acylation and primer extension (SHAPE). *J. Am. Chem. Soc.*, **127**, 4223–4231.
19. Berry,K.E., Waghray,S. and Doudna,J.A. (2010) The HCV IRES pseudoknot positions the initiation codon on the 40S ribosomal subunit. *RNA*, **16**, 1559–1569.
20. Mortimer,S.A. and Weeks,K.M. (2007) A fast-acting reagent for accurate analysis of RNA secondary and tertiary structure by SHAPE chemistry. *J. Am. Chem. Soc.*, **129**, 4144–4145.
21. Mortimer,S.A. and Weeks,K.M. (2009) Time-resolved RNA SHAPE chemistry: quantitative RNA structure analysis in one-second snapshots and at single-nucleotide resolution. *Nat. Protoc.*, **4**, 1413–1421.
22. Witherell,G. (2001) In vitro translation using HeLa extract. *Curr. Protoc. Cell Biol.*, **Chapter 11**, Unit 11.8.
23. Mcginnis,J.L., Duncan,C.D. and Weeks,K.M. (2009) High-throughput SHAPE and hydroxyl radical analysis of RNA structure and ribonucleoprotein assembly. *Methods Enzymol.*, **468**, 67–89.
24. Berry,K.E., Waghray,S., Mortimer,S.A., Bai,Y. and Doudna,J.A. (2011) Crystal structure of the HCV IRES central domain reveals strategy for start-codon positioning. *Structure*, **19**, 1456–1466.
25. Pang,P.S., Pham,E.A., Elazar,M., Patel,S.G., Eckart,M.R. and Glenn,J.S. (2012) Structural map of a microRNA-122: hepatitis C virus complex. *J. Virol.*, **86**, 1250–1254.
26. Dibrov,S.M., Ding,K., Brunn,N.D., Parker,M.A., Bergdahl,B.M., Wyles,D.L. and Hermann,T. (2012) Structure of a hepatitis C virus RNA domain in complex with a translation inhibitor reveals a binding mode reminiscent of riboswitches. *Proc. Natl Acad. Sci.*, **109**, 5223–5228.
27. Henke,J.I., Goergen,D., Zheng,J., Song,Y., Schüttler,C.G., Fehr,C., Jünemann,C. and Niepmann,M. (2008) microRNA-122 stimulates translation of hepatitis C virus RNA. *EMBO J.*, **27**, 3300–3310.
28. Jangra,R.K., Yi,M. and Lemon,S.M. (2010) Regulation of hepatitis C virus translation and infectious virus production by the microRNA miR-122. *J. Virol.*, **84**, 6615–6625.
29. Lukavsky,P.J., Kim,I., Otto,G.A. and Puglisi,J.D. (2003) Structure of HCV IRES domain II determined by NMR. *Nat. Struct. Biol.*, **10**, 1033–1038.
30. Spahn,C.M., Kieft,J.S., Grassucci,R.A., Penczek,P.A., Zhou,K., Doudna,J.A. and Frank,J. (2001) Hepatitis C virus IRES RNA-induced changes in the conformation of the 40s ribosomal subunit. *Science*, **291**, 1959–1962.
31. Boehringer,D., Thermann,R., Ostareck-Lederer,A., Lewis,J.D. and Stark,H. (2005) Structure of the hepatitis C virus IRES bound to the human 80S ribosome: remodeling of the HCV IRES. *Structure*, **13**, 1695–1706.
32. Jinek,M., Coyle,S.M. and Doudna,J.A. (2011) Coupled 5' nucleotide recognition and processivity in Xrn1-mediated mRNA decay. *Mol. Cell*, **41**, 600–608.
33. Takahashi,H., Yamaji,M., Hosaka,M., Kishine,H., Hijikata,M. and Shimotohno,K. (2005) Analysis of the 5' end structure of HCV subgenomic RNA replicated in a Huh7 cell line. *Intervirology*, **48**, 104–111.
34. Li,Y., Masaki,T., Yamane,D., McGivern,D.R. and Lemon,S.M. (2013) Competing and noncompeting activities of miR-122 and the 5' exonuclease Xrn1 in regulation of hepatitis C virus replication. *Proc. Natl Acad. Sci. USA*, **110**, 1881–1886.
35. Wilson,J.A., Zhang,C., Huys,A. and Richardson,C.D. (2011) Human Ago2 is required for efficient microRNA 122 regulation of hepatitis C virus RNA accumulation and translation. *J. Virol.*, **85**, 2342–2350.
36. Roberts,A.P.E., Lewis,A.P. and Jopling,C.L. (2011) miR-122 activates hepatitis C virus translation by a specialized mechanism requiring particular RNA components. *Nucleic Acids Res.*, **39**, 7716–7729.